

Experimental and Numerical Results from Shock Propagation Through Dust Columns in a Shock Tube

M. G. Omang, K. O. Hauge and J. Trulsen

Abstract This chapter presents experimental and numerical work in progress on shock propagation through dust columns in a shock tube environment. The shock tube consists of a short double driver chamber separated by membranes from the driven section. The shock tube is instrumented with pressure sensor and high-speed cameras. A specially designed window section allows Schlieren and shadow photography to be recorded simultaneously, in directions perpendicular to each other. The dust column is injected from below in the driven section, using a spark generator. The timing is such that the dust is in suspension before the shock arrives. The numerical method Regularized Smoothed Particle Hydrodynamics has been used to simulate shock–dust interaction problems, with a full multiphase description. Comparison with experimental data shows promising results for further studies on shock–dust interactions.

1 Introduction

This chapter presents the experimental and numerical work in progress on shock propagation through dust columns in a shock tube environment. A new laboratory is under development at Østøya, close to Horten, Norway, where the experimental work has been performed. The project has been aimed at redesigning the shock tube with a proper window section to allow both optical techniques and pressure sensors to be used.

The numerical work is performed with our in-house code, Regularized Smoothed Particle Hydrodynamics (RSPH), which has been demonstrated to simulate shock–dust interaction problems, with a full multiphase description Omang and Trulsen [6], presenting good results.

M. G. Omang (✉) · J. Trulsen
Institute of Theoretical Astrophysics, University of Oslo, 1029 Blindern, 0315 Oslo, Norway
e-mail: momang@astro.uio.no

M. G. Omang · K. O. Hauge
Norwegian Defence Estates Agency, Forsvarsbygg Futura, 405 Sentrum, 0103 Oslo, Norway
e-mail: knut.ove.hauge@forsvarsbygg.no

Development of numerical methods within this field is dependent on complete and relevant experimental data set, which unfortunately has been difficult to find in the literature, both for inert and reactive particles. Although the results presented here are preliminary, they demonstrate the potential of both the experimental facility and the numerical work, and have already given valuable knowledge for further developments of the experimental setup.

2 Numerical Method

RSPH is a Lagrangian particle interpolation method, where particles are used to simulate a continuous fluid flow. Each particle carries a set of properties, typically mass, pressure, density, velocity, and energy. In multiphase problems, additional properties are introduced, such as the void fraction, θ , describing how dilute the gas-particle distribution is. The smoothing length is the measure of the interaction zone for a given particle. Typically, particles within two smoothing lengths interact with each other in the simulations. A fundamental review on SPH is given in Monaghan [5].

In a multiphase SPH description, each phase has separate sets of particles and a separate set of equations of motion. In the case of nonreactive particles, the two phases are coupled through heat exchange, viscosity, and drag effects. In the present work, the Knudsen and Katz [4] Nusselt number for heat exchange, the dynamic viscosity coefficient from Chapman and Cowling [2], and the Ingebo [3] drag coefficient have been used.

RSPH has two extra functionalities different from regular SPH. First of all, it allows a stepwise variable resolution, in which the smoothing length is allowed to vary in steps of a factor 2. In production simulations, three or four levels of smoothing lengths are typically chosen.

A regularization process is also implemented, which allows the particle distribution to be redistributed at regular time intervals. The regularization is typically carried out every 40–50 time steps. To ensure conservation of mass, momentum, and energy, the particles inherit their properties from the old particle distribution. The regularization process is introduced to optimize the resolution and maintain numerical accuracy over time. A thorough description of RSPH could be found in Borve et al. [1].

3 Experimental Setup

The shock tube consists of a double driver chamber of lengths, $L_{D1} = 0.09$ and $L_{D2} = 0.03$ m, separated by Mylar Dupont membranes from the driven section of $L_{D3} = 8.6$ m. Initially, both driver chambers are pressurized. The first membrane will burst when the pressure in the second chamber is reduced, and the pressure difference between the two driver sections increases above the membrane threshold

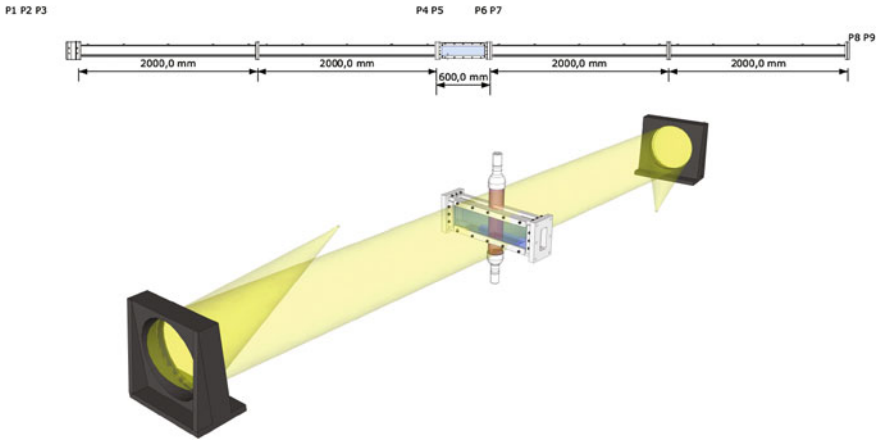


Fig. 1 Upper panel shows a sketch of the shock tube, with positions for pressure sensors P . The lower panel shows a sketch of the optical system. In both panels, the window section glass is illustrated in blue

Table 1 Pressure sensor positions

Test	P_1	P_2	P_3	P_4	P_5	P_6	P_7	P_8	P_9
x [m]	0.015	0.105	0.22	4.22	4.22	4.62	4.62	8.72	8.705
h [m]	0.084	0.084	0.10	0.10	0	0.10	0	0.054	0.10

level. A high degree of repeatability is observed with the use of the double driver chamber facility. The shock tube is illustrated in Fig. 1, with pressure sensor positions $P_{1,2,3,\dots,9}$ included. The exact pressure sensor positions are given in Table 1. Preliminary tests to reduce the pressure in the driven section have also been investigated, as this technique could extend the experimental Mach number range as well as increase the temperature, which is important for shock ignition of reactive particles.

A specially designed window section allows Schlieren and shadow photography to be recorded simultaneously, in directions perpendicular to each other. The system is illustrated in the sketch of Fig. 1. A Z-type Schlieren system is set up, with parabolic mirrors of diameter 317.5 mm and effective focal length of 2540 mm used together with a Cree XM-L Led lamp. As illustrated in Fig. 1, the shadow photography technique is mounted in the vertical direction. The dust column is injected from below, at $x = 4.442$ m, using a spark generator. The dust consists of aluminum-coated barium titanate solid glass microspheres manufactured by Cospheric. The glass particles have a density of 4490 kg/m^3 , and a mean diameter size of $40\text{--}50 \text{ }\mu\text{m}$. The timing is such that the dust is in suspension before the shock arrives. The image from the second parabolic mirror is focused on a knife-edge and captured with a Phantom Miro 310 high-speed camera using a Nikkor 70–200 mm 2.8 lens. A frame rate of 8680 frames per second is used.

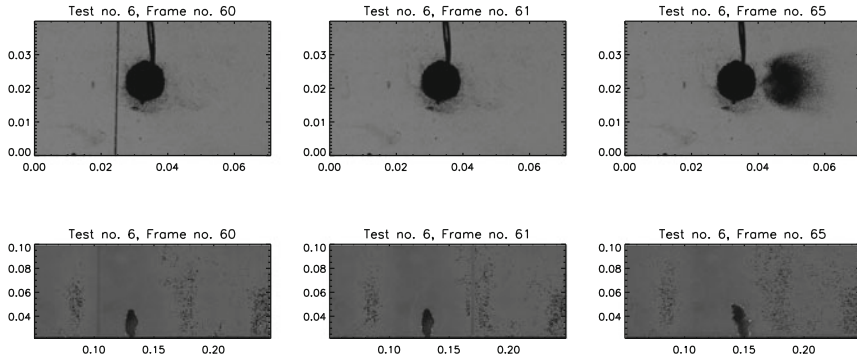


Fig. 2 High-speed video of a shock propagating through a dust column. The upper panel shows the shadow photography as observed from above. The lower panel shows the results from the Schlieren photography, as observed from the side

Test results of the high-speed video are illustrated in Fig. 2. The upper panel shows the video from the shadow photography as observed from above. In the first two frames, it is difficult to distinguish the dust, which has been injected from below, from the injection system, consisting of a black circular disk and cable. The left panel shows the situation right before the shock arrives at the dust cloud. The shock is observed as a black vertical line. In the next frame, the shock has passed through the cloud, and out of the picture, but the dust cloud has not moved significantly yet and is still difficult to observe. The last picture shows the same situation 4 frames, or 0.46 ms later. Here, the dust cloud clearly has moved to the right, relative to the initial position. The circular shape of the cloud is worth noticing.

In the lower panel of Fig. 2, the results from the Schlieren photography technique are presented, with a larger field of view. In the left panel, the dust column is observed prior to shock passage, with the shock visible to the left of the cloud. The next panel illustrates the situation right after shock passage. At this time, the dust column has not moved significantly yet, whereas in the right panel, we observe how the dust has been accelerated and moved to the right relative to the previous results. For these preliminary experimental results, the synchronization of the two high-speed cameras are within or less than one picture cycle time. For the experiment presented in Fig. 2, there is a synchronization difference of approximately one-third of a picture cycle time.

4 Results Presentation and Discussion

The initial conditions of the numerical simulations are determined from the pressure gauges in the two driver sections. In these preliminary test, the temperature is measured for the atmospheric conditions in the room, only. In Table 2, the densities given

Table 2 Initial conditions for the numerical simulations

Test no.	P_0 [kPa]	P_1 [kPa]	P_2 [kPa]	ρ_0 [m/kg ³]	ρ_1 [m/kg ³]	ρ_2 [m/kg ³]	ρ_d	θ_d	d_d [μ m]
4	100.01	167.53	980.52	1.203	1.8	10.0	2702	0.0005	6
6	32.47	165.100	998.36	0.4134	1.8	10.0	4490	0.0005	40

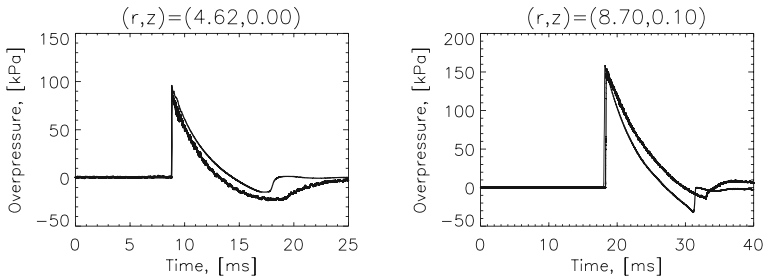


Fig. 3 Experimental and numerical pressure–time histories downstream of the window section for two different sensor positions

in the two driver sections are, therefore, based on assumptions relating the external and internal temperatures. The void fraction has so far been difficult to determine experimentally. Techniques to determine the void fraction are currently being evaluated. In Fig. 3, pressure sensor measurements downstream of the window section is plotted for both numerical and experimental results, the experimental results with the thicker line style. Results are presented for two different positions, $x = 4.62$ m and $x = 8.70$ m. As the figure illustrates, both time of arrival and pressure levels show good agreement with the experimental results.

Numerical simulations were also performed to study shock interaction with the dust cloud. Figure 4 shows a density contour plot of the dust cloud, plotted in x-y coordinates. In the results presented here, a dust particle diameter of 40 μ m was chosen, as this choice was found to give the best agreement with the experimental data. The dust cloud position was determined manually from the high-speed Schlieren pictures and has been plotted on top with a black contour line. The plot illustrates the situation for two different time steps, $t = 6.4$ ms and $t = 7.1$ ms after membrane rupture.

In the current work, only one-size dust particles were assumed, described with a constant smoothing length. In the real experiments, the particles had a mean size of 40–50 μ m, but particles of other sizes were also present in the distribution, although fewer. The specifications for the particles indicate a size range from 32 to 80 μ m. Introducing particles of different sizes in the simulations, also implies introducing one phase for each particle size, this would be possible, but quite time-consuming. Although the results presented here were based on relatively low-resolution simulations, using 270 dust particles, and gas simulation particles starting at approximately

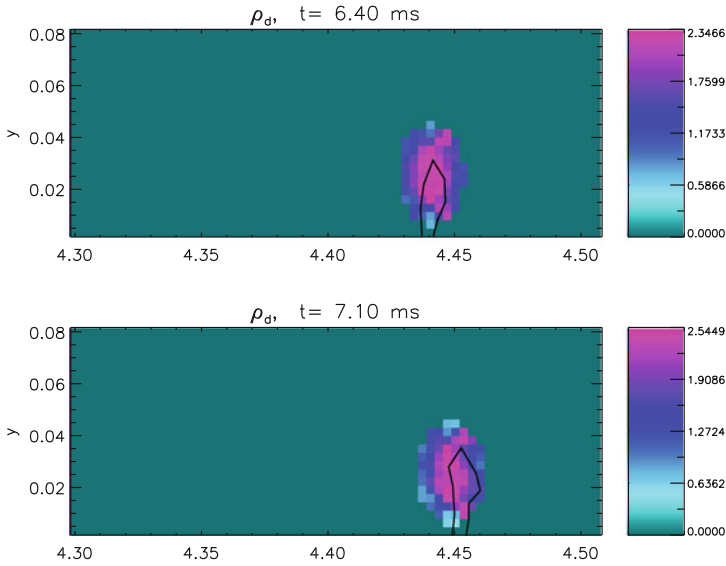


Fig. 4 Numerical simulations of the dust column at two different time steps, before and after shock interaction. The black contour line illustrates the position of the cloud captured manually from the Schlieren high-speed video

60000, and increasing to 400000 at the end, the results show good agreement and are promising for further studies on shock–dust interactions.

References

1. Børve, S., Omang, M., Trulsen, J.: Regularized smoothed particle hydrodynamics with improved multi-resolution handling. *J. Comput. Phys.* **208**(1), 345–367 (2005)
2. Chapman, S., Cowling, T.G.: *The Mathematical Theory of Non-uniform Gases*. Cambridge University Press (1961)
3. Ingebo, R.D.: Drag coefficients for droplets and solid spheres in clouds accelerating in air streams. Technical Report No. TN 3762, NACA Technical Note TN (1956)
4. Knudsen, J., Katz, D.: *Fluid Mechanics And Heat Transfer*. McGraw-Hill, New York (1958)
5. Monaghan, J.J.: Smoothed particle hydrodynamics. *Rep. Prog. Phys.* **68**(8), 1703–1759 (2005)
6. Omang, M., Trulsen, J.: Multi-phase shock simulations with Smoothed Particle Hydrodynamics (SPH). *Shock Waves* **24**(5), 521–536 (2014)